전남대학교
CHONNAM NATIONAL UNIVERSITY

Quantum Entanglement and Bell nonlocality in top-quark pair production at a photon linear collider

Jae Sik Lee (Chonnam Nat'l Univ.)

The 8th mini-workshop on Chirality in the Universe Beyond the Electroweak Scale (CUBES 2026)
24-26 April 2026, The K Jirisan Family Hotel, Sandong, Gurye

arXiv: 2603.12830,

a work in collaboration with S.Y. Choi (JBNU), D.W. Kang (JBNU), and C.B. Park (CNU)

Contents:

Quantum entanglement

Quantum entanglement gives rise to the stronger spin correlations than those expected in the classical theory, among the states which once interacted but, being separated spatially, cannot interact now.

At colliders, the measurement takes place when the polarized particles decay and quantum entanglement is accessible through correlations among particle spins.

At colliders, the spin correlations are accessible through the distribution of the momenta of the final states into which the entangled particles decay

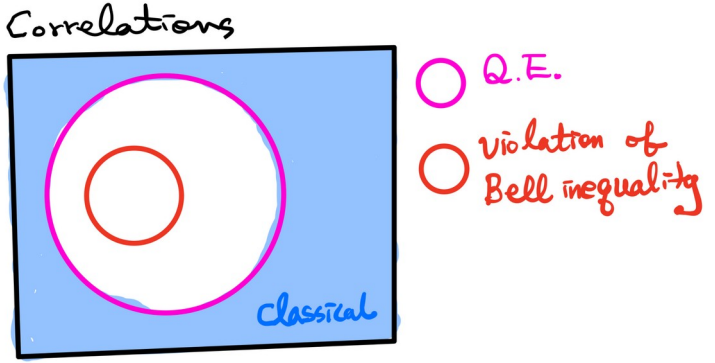

Quantum entanglement and Bell inequality violation at colliders #1

Alan J. Barr (Oxford U. and Merton Coll., Oxford), Marco Fabbrichesi (INFN, Trieste), Roberto Floreanini (INFN, Trieste), Emidio Gabrielli (INFN, Trieste and NICPB, Tallinn), Luca Marzola (NICPB, Tallinn) (Feb 12, 2024)

Published in: *Prog.Part.Nucl.Phys.* 139 (2024) 104134 • e-Print: 2402.07972 [hep-ph]

pdf DOI cite claim reference search 120 citations

At the LHC:

near the $t\bar{t}$ production threshold

Observation of quantum entanglement with top quarks at the ATLAS detector #1

ATLAS Collaboration • Georges Aad (Marseille, CPPM) et al. (Nov 13, 2023)

Published in: *Nature* 633 (2024) 8030, 542-547 • e-Print: 2311.07288 [hep-ex]

pdf links DOI cite claim reference search 257 citations

Observation of quantum entanglement in top quark pair production in proton–proton collisions at $\sqrt{s} = 13$ TeV #1

CMS Collaboration • Aram Hayrapetyan (Yerevan Phys. Inst.) et al. (Jun 6, 2024)

Published in: *Rept.Prog.Phys.* 87 (2024) 11, 117801, *Rept.Prog.Phys.* 87 (2024) 117801 • e-Print: 2406.03976 [hep-ex]

pdf DOI cite datasets claim reference search 160 citations

at high $t\bar{t}$ invariant masses

Measurements of polarization and spin correlation and observation of entanglement in top quark pairs using $\mathrm{lepton} + \mathrm{jets}$ events from proton-proton collisions at $\sqrt{s} = 13$ TeV #1

CMS Collaboration • Aram Hayrapetyan (Yerevan Phys. Inst.) et al. (Sep 17, 2024)

Published in: *Phys.Rev.D* 110 (2024) 11, 112016 • e-Print: 2409.11067 [hep-ex]

pdf DOI cite datasets claim reference search 79 citations

… with a significance exceeding 5σ

Entanglement quantifiers

The spin density matrix of a two-qubit system which describes production of a pair of top-antitop quarks:

1 (normalization : Tr[rho] = 1)

+ 6 (polarizations) + 9 (spin correlations) = 16

$$\rho = \frac{1}{4}\left[\mathbf{1}_2 \otimes \mathbf{1}_2 + \sum_{i=1}^{3} B_i^+ \left(\sigma_i \otimes \mathbf{1}_2\right) + \sum_{j=1}^{3} B_j^- \left(\mathbf{1}_2 \otimes \sigma_j\right) + \sum_{i,j=1}^{3} C_{ij} \left(\sigma_i \otimes \sigma_j\right)\right]$$

$$\mathbf{1}_2 = \begin{pmatrix} 1 & 0 \\ 0 & 1 \end{pmatrix};\ \sigma_1 = \begin{pmatrix} 0 & 1 \\ 1 & 0 \end{pmatrix},\ \sigma_2 = \begin{pmatrix} 0 & -i \\ i & 0 \end{pmatrix},\ \sigma_3 = \begin{pmatrix} 1 & 0 \\ 0 & -1 \end{pmatrix}.$$

Given the spin density matrix, quantum entanglement and violation of the Bell inequality can be readily evaluated !

Peres-Horodecki criterion : Negativity

$$\rho^{T_B} = (\mathbf{1}_A \otimes T_B)[\rho] < 0 \iff \text{entangled} \qquad \mathcal{N}[\rho] = \sum_k \frac{|\lambda_k| - \lambda_k}{2} = \sum_{\lambda_k<0} |\lambda_k| \,,$$

Concurrence $\mathcal{C}[\rho] = \max(0, r_1 - r_2 - r_3 - r_4) > 0 \iff \text{entangled}\,,$

r1,2,3,4 with r1 ≥ r2,3,4 are the square roots of nonnegative eigenvalues of

$$R = \rho\,(\sigma_2 \otimes \sigma_2)\,\rho^*\,(\sigma_2 \otimes \sigma_2)\,,$$

Clauser-Horne-Shimony-Holt (CHSH) inequality + Horodecki condition m12

$$m_{12} \equiv m_1 + m_2 > 1 \iff \text{violation of Bell inequality}\,,$$

m1 ≥ m2 ≥ m3 are the three eigenvalues of the symmetric matrix

$$M = CC^T\,,$$

C : the 3 × 3 spin correlation matrix appearing in

$$\rho = \frac{1}{4}\left[\mathbf{1}_2 \otimes \mathbf{1}_2 + \sum_{i=1}^{3} B_i^+\,(\sigma_i \otimes \mathbf{1}_2) + \sum_{j=1}^{3} B_j^-\,(\mathbf{1}_2 \otimes \sigma_j) + \sum_{i,j=1}^{3} C_{ij}\,(\sigma_i \otimes \sigma_j)\right]$$

Entanglement marker D

$$D \equiv \frac{1}{3}\Delta_E < -\frac{1}{3} \implies \text{entangled}, \quad \Delta_E = C_{11} - |C_{22} + C_{33}|.$$

D = Tr[C]/3 when the diagonal components of the 3 × 3 correlation matrix C are all negative

... adopted by ATLAS & CMS near the $t\bar{t}$ threshold

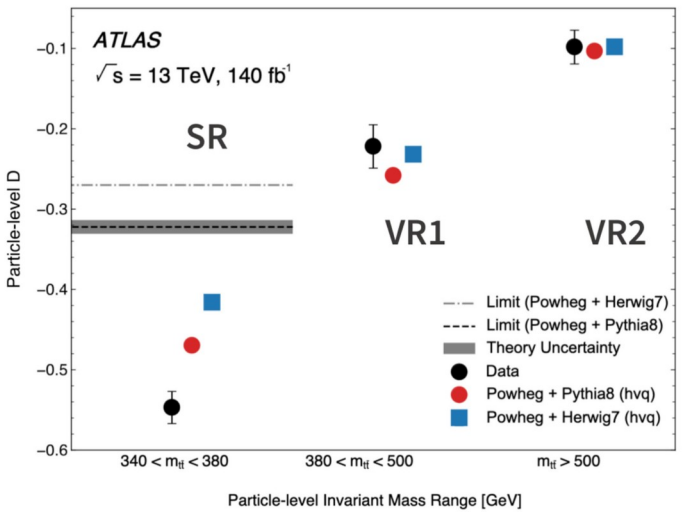

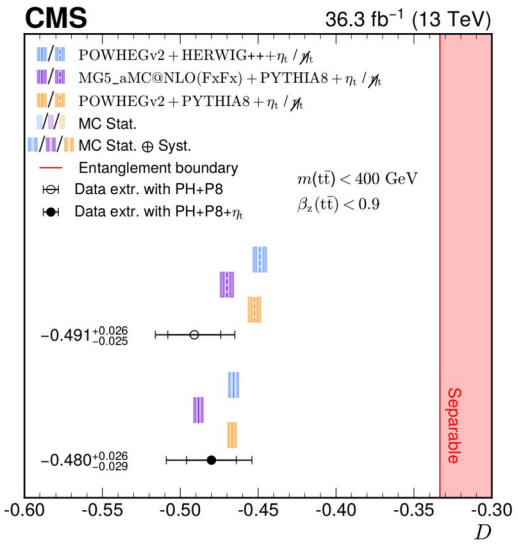

$D = -0.537 \pm 0.002\,(\text{stat.}) \pm 0.019\,(\text{syst.})$ for $340 < m_{t\bar{t}} < 380$ GeV

$D = -0.480^{+0.016}_{-0.017}\,(\text{stat})\,^{+0.020}_{-0.023}\,(\text{syst})$

(repeat) Given the spin density matrix, quantum entanglement and violation of the Bell inequality can be readily evaluated by calculating Negativity N, Concurrence C, Bell nonlocality parameter m12, and/or Entanglement marker D !

⋯ then how to calculate the spin density matrix ?

$$\rho = \frac{1}{4}\left[\mathbf{1}_2 \otimes \mathbf{1}_2 + \sum_{i=1}^{3} B_i^{+}\left(\sigma_i \otimes \mathbf{1}_2\right) + \sum_{j=1}^{3} B_j^{-}\left(\mathbf{1}_2 \otimes \sigma_j\right) + \sum_{i,j=1}^{3} C_{ij}\left(\sigma_i \otimes \sigma_j\right)\right]$$

Spin density matrix of a two-qubit system

Process: $\gamma(k_1,\lambda_1) + \gamma(k_2,\lambda_2) \rightarrow t(p,\sigma) + \bar{t}(\bar{p},\bar{\sigma})\,,$

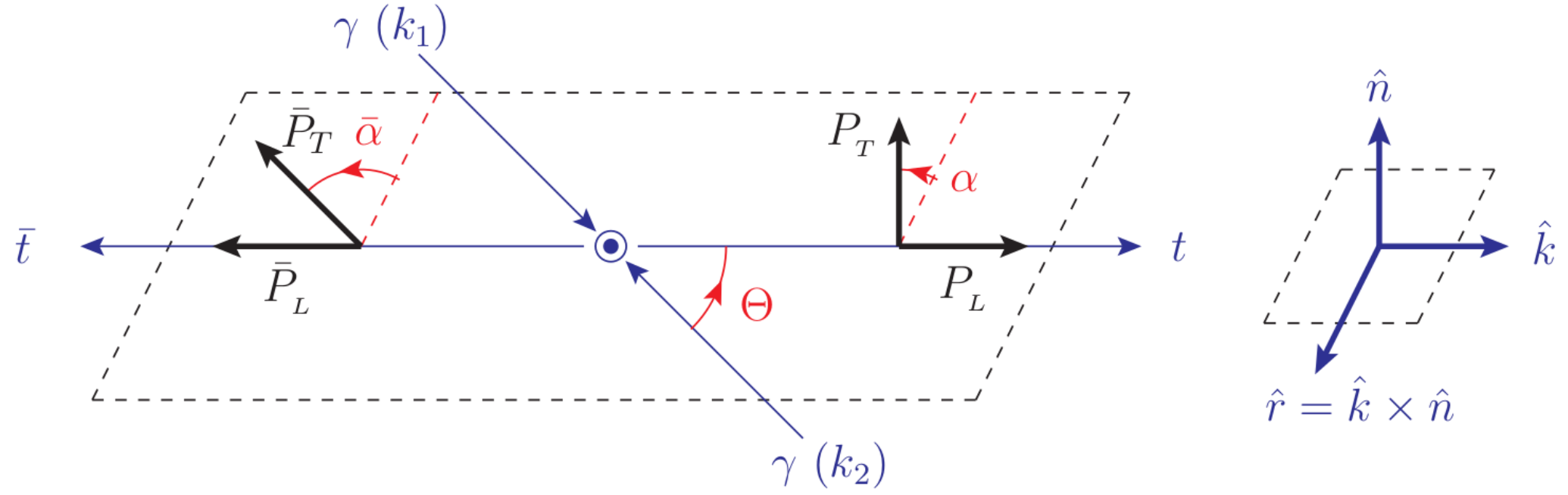

Helicity amplitude: $\gamma(k_1,\lambda_1) + \gamma(k_2,\lambda_2) \;\to\; t(p,\sigma) + \bar{t}(\bar{p},\bar{\sigma})\,,$

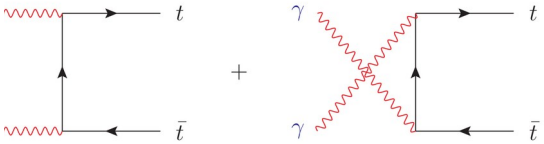

$$\mathcal{M}_{\lambda_1\lambda_2;\sigma\bar{\sigma}} \equiv \mathcal{A}_C\,\langle\sigma\bar{\sigma};\lambda_1\lambda_2\rangle = \frac{8\pi\alpha Q_t^2}{1-\beta^2\cos^2\Theta}\,\langle\sigma\bar{\sigma};\lambda_1\lambda_2\rangle \;\text{ with }\; \mathcal{A}_C = \frac{8\pi\alpha Q_t^2}{1-\beta^2\cos^2\Theta}\,,$$

TABLE I. The reduced amplitudes $\langle\sigma\bar{\sigma};\lambda_1\lambda_2\rangle$ in Eq. (15). Here, $\beta = \sqrt{1-4M_t^2/\hat{s}}$, where M_t denotes the pole mass of the top quark, and Θ is the angle between $\vec{k}_1$ and $\vec{p}$ in the production plane (see Fig. 1).

$(\lambda_1\lambda_2)\downarrow\ (\sigma\bar{\sigma})\to$	$\langle{+}{+}\rangle$	$\langle{-}{-}\rangle$	$\langle{-}{+}\rangle$	$\langle{+}{-}\rangle$
$\langle{+}{+}\rangle$	$\frac{2M_t}{\sqrt{\hat{s}}}\,[1+\beta]$	$\frac{2M_t}{\sqrt{\hat{s}}}\,[1-\beta]$	0	0
$\langle{-}{-}\rangle$	$\frac{2M_t}{\sqrt{\hat{s}}}\,[-1+\beta]$	$\frac{2M_t}{\sqrt{\hat{s}}}\,[-1-\beta]$	0	0
$\langle{-}{+}\rangle$	$-\frac{2M_t}{\sqrt{\hat{s}}}\beta\,\sin^2\Theta$	$\frac{2M_t}{\sqrt{\hat{s}}}\beta\,\sin^2\Theta$	$-\beta\sin\Theta\,(\cos\Theta+1)$	$-\beta\sin\Theta\,(\cos\Theta-1)$
$\langle{+}{-}\rangle$	$-\frac{2M_t}{\sqrt{\hat{s}}}\beta\,\sin^2\Theta$	$\frac{2M_t}{\sqrt{\hat{s}}}\beta\,\sin^2\Theta$	$-\beta\sin\Theta\,(\cos\Theta-1)$	$-\beta\sin\Theta\,(\cos\Theta+1)$

Spin density matrix in the n-r-k basis: Results

$$\rho = \frac{1}{4}\left[\mathbf{1}_2 \otimes \mathbf{1}_2 + \frac{1}{\widehat{A}} \sum_{i=n,r,k} \widehat{B}_i^{+} \left(\sigma_i \otimes \mathbf{1}_2\right) + \frac{1}{\widehat{A}} \sum_{j=n,r,k} \widehat{B}_j^{-} \left(\mathbf{1}_2 \otimes \sigma_j\right) + \frac{1}{\widehat{A}} \sum_{i,j=n,r,k} \widehat{C}_{ij} \left(\sigma_i \otimes \sigma_j\right)\right]$$

$$\widehat{A} = \widehat{C}_1[+++] + \widehat{C}_3[+++]\,,$$

$$\widehat{B}_i^{+} = \left(\widehat{C}_6[++-] + \widehat{C}_8[+-+], -\widehat{C}_5[-++] - \widehat{C}_7[---], \widehat{C}_2[---] + \widehat{C}_4[-++]\right),$$

$$\widehat{B}_j^{-} = \left(\widehat{C}_6[++-] - \widehat{C}_8[+-+], -\widehat{C}_5[-++] + \widehat{C}_7[---], -\widehat{C}_2[---] + \widehat{C}_4[-++]\right),$$

$$\widehat{C}_{ij} = \begin{pmatrix} \widehat{C}_{13}[+++] - \widehat{C}_{15}[+++] & -\widehat{C}_{14}[--+] - \widehat{C}_{16}[-+-] & -\widehat{C}_{10}[--+] - \widehat{C}_{12}[-+-] \\ \widehat{C}_{14}[--+] - \widehat{C}_{16}[-+-] & \widehat{C}_{13}[+++] + \widehat{C}_{15}[+++] & \widehat{C}_9[+--] + \widehat{C}_{11}[+++] \\ \widehat{C}_{10}[--+] - \widehat{C}_{12}[-+-] & -\widehat{C}_9[+--] + \widehat{C}_{11}[+++] & -\widehat{C}_1[+++] + \widehat{C}_3[+++] \end{pmatrix}$$

The hatted 16 polarizations coefficients in terms of the reduced amplitudes:

$$\widehat{C}_1[+++] = \frac{1}{4}\sum_{\lambda_1,\lambda_2=\pm}\left[|\langle{+}{+};\lambda_1\lambda_2\rangle|^2+|\langle{-}{-};\lambda_1\lambda_2\rangle|^2\right],$$

$$\widehat{C}_2[---] = \frac{1}{4}\sum_{\lambda_1,\lambda_2=\pm}\left[|\langle{+}{+};\lambda_1\lambda_2\rangle|^2-|\langle{-}{-};\lambda_1\lambda_2\rangle|^2\right],$$

$$\widehat{C}_3[+++] = \frac{1}{4}\sum_{\lambda_1,\lambda_2=\pm}\left[|\langle{-}{+};\lambda_1\lambda_2\rangle|^2+|\langle{+}{-};\lambda_1\lambda_2\rangle|^2\right],$$

$$\widehat{C}_4[-++] = -\frac{1}{4}\sum_{\lambda_1,\lambda_2=\pm}\left[|\langle{-}{+};\lambda_1\lambda_2\rangle|^2-|\langle{+}{-};\lambda_1\lambda_2\rangle|^2\right],$$

$$\widehat{C}_5[-++] = \frac{1}{4}\,\Re\mathrm{e}\sum_{\lambda_1,\lambda_2=\pm}\big(\langle{+}{+};\lambda_1\lambda_2\rangle-\langle{-}{-};\lambda_1\lambda_2\rangle\big)\big(\langle{-}{+};\lambda_1\lambda_2\rangle-\langle{+}{-};\lambda_1\lambda_2\rangle\big)^*,$$

$$\widehat{C}_6[++-] = -\frac{1}{4}\,\Im\mathrm{m}\sum_{\lambda_1,\lambda_2=\pm}\big(\langle{+}{+};\lambda_1\lambda_2\rangle-\langle{-}{-};\lambda_1\lambda_2\rangle\big)\big(\langle{-}{+};\lambda_1\lambda_2\rangle+\langle{+}{-};\lambda_1\lambda_2\rangle\big)^*,$$

$$\widehat{C}_7[---] = \frac{1}{4}\,\Re\mathrm{e}\sum_{\lambda_1,\lambda_2=\pm}\big(\langle{+}{+};\lambda_1\lambda_2\rangle+\langle{-}{-};\lambda_1\lambda_2\rangle\big)\big(\langle{-}{+};\lambda_1\lambda_2\rangle+\langle{+}{-};\lambda_1\lambda_2\rangle\big)^*,$$

$$\widehat{C}_8[+-+] = -\frac{1}{4}\,\Im\mathrm{m}\sum_{\lambda_1,\lambda_2=\pm}\big(\langle{+}{+};\lambda_1\lambda_2\rangle+\langle{-}{-};\lambda_1\lambda_2\rangle\big)\big(\langle{-}{+};\lambda_1\lambda_2\rangle-\langle{+}{-};\lambda_1\lambda_2\rangle\big)^*,$$

$$\widehat{C}_9[+--] = \frac{1}{4}\,\Re\mathrm{e}\sum_{\lambda_1,\lambda_2=\pm}\big(\langle{+}{+};\lambda_1\lambda_2\rangle+\langle{-}{-};\lambda_1\lambda_2\rangle\big)\big(\langle{-}{+};\lambda_1\lambda_2\rangle-\langle{+}{-};\lambda_1\lambda_2\rangle\big)^*,$$

$$\widehat{C}_{10}[--+] = -\frac{1}{4}\,\Im\mathrm{m}\sum_{\lambda_1,\lambda_2=\pm}\big(\langle{+}{+};\lambda_1\lambda_2\rangle+\langle{-}{-};\lambda_1\lambda_2\rangle\big)\big(\langle{-}{+};\lambda_1\lambda_2\rangle+\langle{+}{-};\lambda_1\lambda_2\rangle\big)^*,$$

$$\widehat{C}_{11}[+++] = \frac{1}{4}\,\Re\mathrm{e}\sum_{\lambda_1,\lambda_2=\pm}\big(\langle{+}{+};\lambda_1\lambda_2\rangle-\langle{-}{-};\lambda_1\lambda_2\rangle\big)\big(\langle{-}{+};\lambda_1\lambda_2\rangle+\langle{+}{-};\lambda_1\lambda_2\rangle\big)^*,$$

$$\widehat{C}_{12}[-+-] = -\frac{1}{4}\,\Im\mathrm{m}\sum_{\lambda_1,\lambda_2=\pm}\big(\langle{+}{+};\lambda_1\lambda_2\rangle-\langle{-}{-};\lambda_1\lambda_2\rangle\big)\big(\langle{-}{+};\lambda_1\lambda_2\rangle-\langle{+}{-};\lambda_1\lambda_2\rangle\big)^*,$$

$$\widehat{C}_{13}[+++] = -\frac{1}{2}\,\Re\mathrm{e}\sum_{\lambda_1,\lambda_2=\pm}\left[\langle{+}{+};\lambda_1\lambda_2\rangle\langle{-}{-};\lambda_1\lambda_2\rangle^*\right],$$

$$\widehat{C}_{14}[--+] = \frac{1}{2}\,\Im\mathrm{m}\sum_{\lambda_1,\lambda_2=\pm}\left[\langle{+}{+};\lambda_1\lambda_2\rangle\langle{-}{-};\lambda_1\lambda_2\rangle^*\right],$$

$$\widehat{C}_{15}[+++] = -\frac{1}{2}\,\Re\mathrm{e}\sum_{\lambda_1,\lambda_2=\pm}\left[\langle{-}{+};\lambda_1\lambda_2\rangle\langle{+}{-};\lambda_1\lambda_2\rangle^*\right],$$

$$\widehat{C}_{16}[-+-] = -\frac{1}{2}\,\Im\mathrm{m}\sum_{\lambda_1,\lambda_2=\pm}\left[\langle{-}{+};\lambda_1\lambda_2\rangle\langle{+}{-};\lambda_1\lambda_2\rangle^*\right].$$

unpolarized differential cross section

$$\mathrm{d}\hat{\sigma}_0 = \frac{1}{2\hat{s}}\,N_c\,\overline{\sum|\mathcal{M}|^2}\,\mathrm{d}\Phi_2 = \frac{1}{2\hat{s}}\,N_c\left[\frac{|\mathcal{A}_C|^2}{4}\sum_{\lambda_1,\lambda_2,\sigma,\bar{\sigma}}|\langle\sigma\bar{\sigma};\lambda_1\lambda_2\rangle|^2\right]\frac{\beta}{16\pi}\,\mathrm{d}\cos\Theta = \frac{\beta\,N_c}{32\pi\hat{s}}\,|\mathcal{A}_C|^2\,\widehat{A}\,\mathrm{d}\cos\Theta\,,$$

Explicitly:

$$\rho = \frac{1}{4}\left[\mathbf{1}_2 \otimes \mathbf{1}_2 + \frac{1}{\widehat{A}} \sum_{i=n,r,k} \widehat{B}_i^+ \left(\sigma_i \otimes \mathbf{1}_2\right) + \frac{1}{\widehat{A}} \sum_{j=n,r,k} \widehat{B}_j^- \left(\mathbf{1}_2 \otimes \sigma_j\right) + \frac{1}{\widehat{A}} \sum_{i,j=n,r,k} \widehat{C}_{ij} \left(\sigma_i \otimes \sigma_j\right)\right]$$

$$= \frac{1}{4}\left(\begin{array}{cc|cc} 1+B_3^+ + B_3^- + C_{33} & B_1^- + C_{31} - i(B_2^- + C_{32}) & B_1^+ + C_{13} - i(B_2^+ + C_{23}) & C_{11} - C_{22} - i(C_{12} + C_{21}) \\ B_1^- + C_{31} + i(B_2^- + C_{32}) & 1 + B_3^+ - B_3^- - C_{33} & C_{11} + C_{22} + i(C_{12} - C_{21}) & B_1^+ - C_{13} - i(B_2^+ - C_{23}) \\ \hline B_1^+ + C_{13} + i(B_2^+ + C_{23}) & C_{11} + C_{22} + i(C_{21} - C_{12}) & 1 - B_3^+ + B_3^- - C_{33} & B_1^- - C_{31} - i(B_2^- - C_{32}) \\ C_{11} - C_{22} + i(C_{21} + C_{12}) & B_1^+ - C_{13} + i(B_2^+ - C_{23}) & B_1^- - C_{31} + i(B_2^- - C_{32}) & 1 - B_3^+ - B_3^- + C_{33} \end{array}\right)$$

We have developed the amplitude-level formalism for a spin density matrix of a two-qubit system which is almost process- and model-independent and applicable to other processes and to new-physics searches beyond the SM. It also helps to classify the spin density matrix by P, CP, and CPT~ parities.

Photon collider : not dead !

Even recently….

XCC: An X-ray FEL-based $\gamma\gamma$ Compton Collider Higgs Factory #1

T. Barklow (SLAC), C. Emma (SLAC), Z. Huang (SLAC), A. Naji (SLAC), E. Nanni (SLAC) et al. (Jun 14, 2023)

Published in: *JINST* 18 (2023) 07, P07028 • e-Print: 2306.10057 [physics.acc-ph]

pdf DOI cite claim reference search 15 citations

A Linear Collider Vision for the Future of Particle Physics #1

Linear Collider Vision Collaboration • H. Abramowicz (Tel Aviv U.) et al. (Mar 25, 2025)

Published in: *Eur.Phys.J.ST* (2026) • e-Print: 2503.19983 [hep-ex]

pdf links DOI cite claim reference search 94 citations

The Linear Collider Facility (LCF) at CERN #1

Linear Collider Collaboration • H. Abramowicz (Tel Aviv U.) et al. (Mar 31, 2025)

e-Print: 2503.24049 [hep-ex]

pdf links cite claim reference search 48 citations

A photon linear collider, the two-photon collision mode of an e+ e− linear collider, uses high-energy laser photons backscattered off the incoming electrons and positrons.

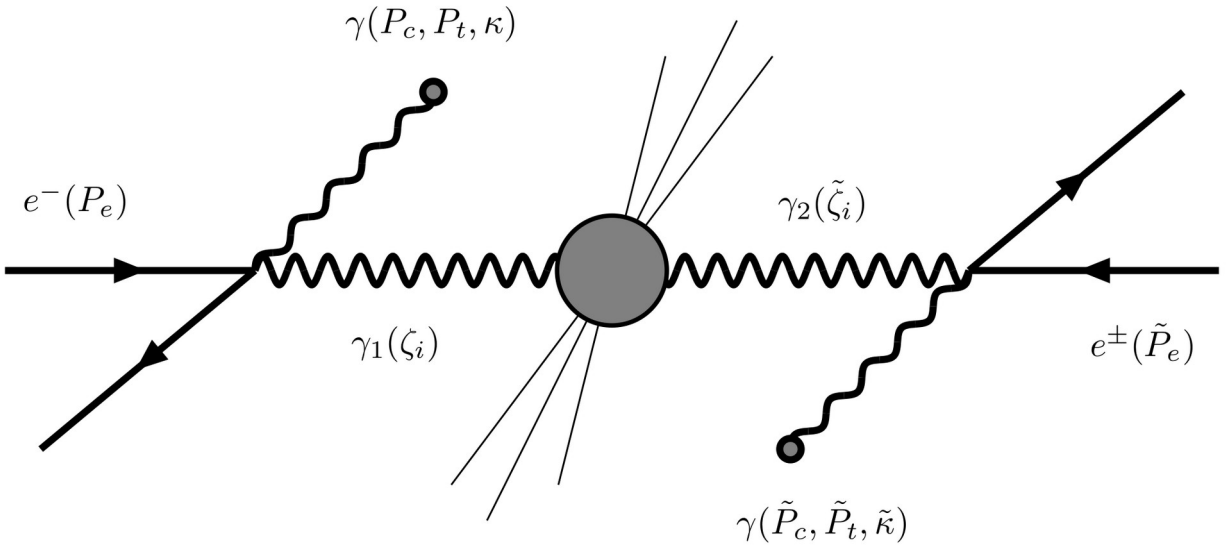

$$y_i \equiv E_{\gamma_i} / E_b$$

$$y_{\max} = x/(1+x)$$

$$x = \frac{4\, E_b\, \omega_0}{m_e^2} = 15.3 \left(\frac{E_b}{\mathrm{TeV}}\right)\left(\frac{\omega_0}{\mathrm{eV}}\right)$$

Machine parameter

Fig. 1. *Schematic diagram of a $\gamma\gamma$ collider. Polarizations of the initial electron and positron beams are denoted by P_e and $\tilde{P}_e$, respectively. For initial laser photons: P_c and $\tilde{P}_c$ are degrees of circular polarization or mean photon helicity, P_t and $\tilde{P}_t$ the degrees of linear polarization, and κ and $\tilde{\kappa}$ the azimuthal angles of the direction of the maximum linear polarizations. The mean polarizations of the colliding photon beams are denoted by the Stokes parameters ζ_i and $\tilde{\zeta}_i$, see Eq. (8).*

Probing Higgs-sector CP violation at a photon collider

Jae Sik Lee (Seoul Natl. U.) (May, 2007)

Published in: *Mod.Phys.Lett.A* 22 (2007) 1191-1208 • e-Print: 0705.1089 [hep-ph]

The photon-photon luminosity

$$\frac{1}{\mathcal{L}_{ee}}\frac{\mathrm{d}\mathcal{L}_{\gamma\gamma}}{\mathrm{d}\tau} = \int_{\tau/y_{\max}}^{y_{\max}} \frac{\mathrm{d}y'}{y'} f(y') f(\tau/y')$$

where $\tau \equiv \hat{s}/s$ with $\hat{s}$ being the c.m. energy of colliding photons γ1 and γ2

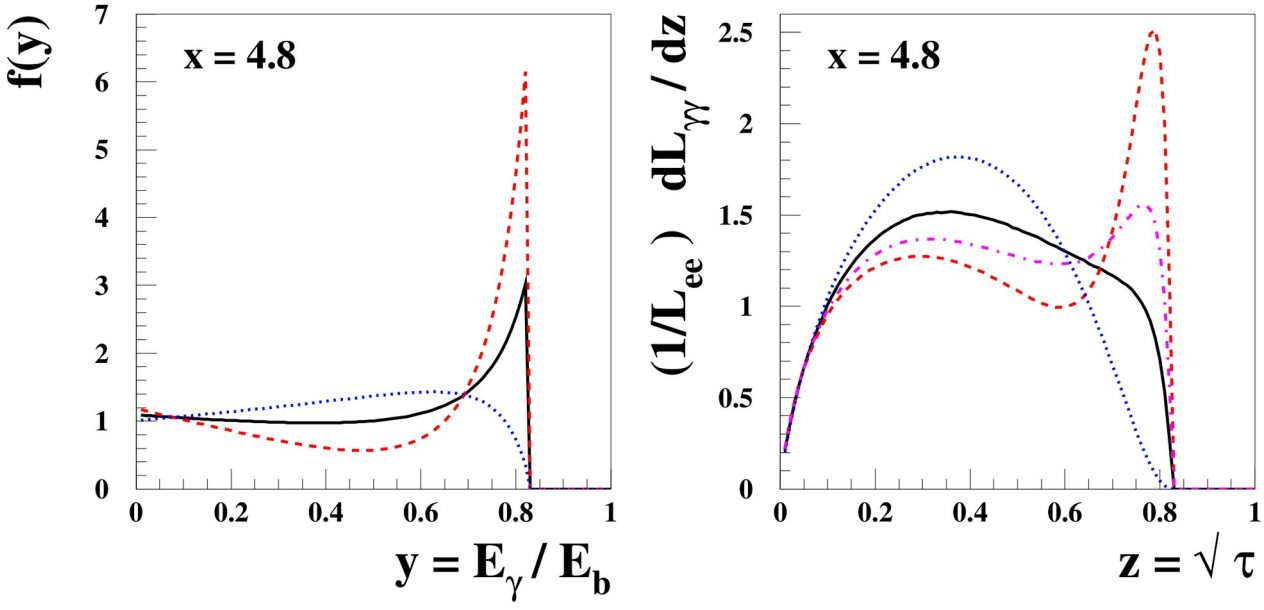

$$P_e P_c = \tilde{P}_e \tilde{P}_c = -1$$

Fig. 2. *Photon energy spectrum (left frame) and spectral luminosity of $\gamma\gamma$ collisions (right frame). In the left frame, the solid black line is for $P_e \cdot P_c = 0$, the dashed red line for $P_e \cdot P_c = -1$, and the dotted blue line for $P_e \cdot P_c = 1$. In the right frame, $(P_e \cdot P_c, \widetilde{P}_e \cdot \widetilde{P}_c) = (0,0)$, $(-1,-1)$, $(1,1)$, and $(0,-1)$ for the solid black, dashed red, dotted blue, and dash-dotted magenta lines, respectively.*

$$P_e P_c = \tilde{P}_e \tilde{P}_c = -1$$

$$L^{\lambda_1\lambda_2} \equiv \frac{1}{\mathcal{L}_{ee}} \frac{\mathrm{d}\mathcal{L}_{\gamma\gamma}^{\lambda_1\lambda_2}}{\mathrm{d}\sqrt{\tau}}$$

Helicity-dependent luminosities: peaks near sqrt(τ) ≃ 0.8 when (λ1 , λ2) = (Pe , P̃e) !!!

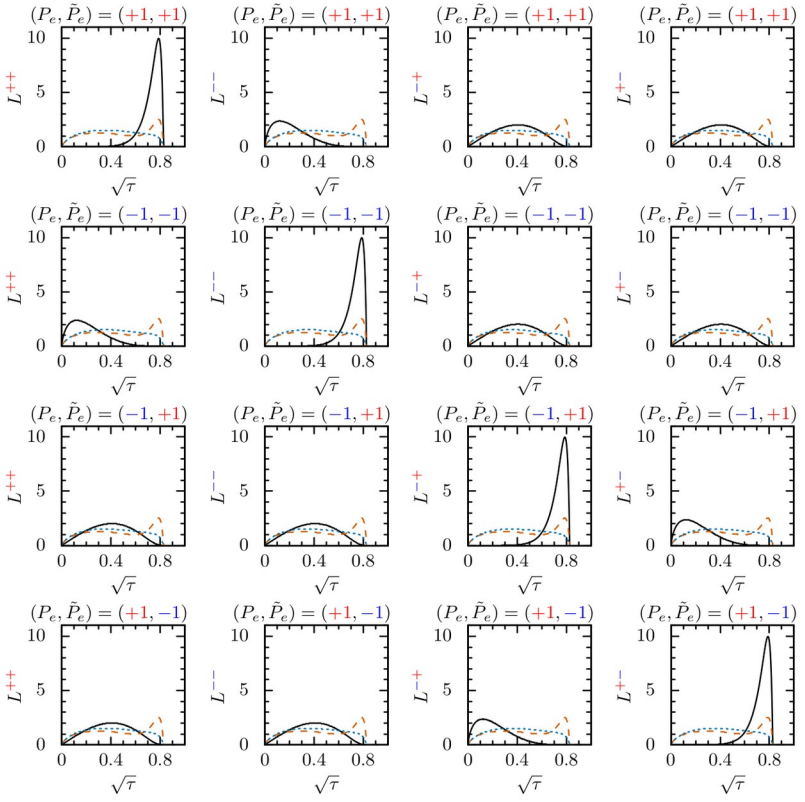

weight functions

$$w^{\lambda_1\lambda_2} \equiv \frac{L^{\lambda_1\lambda_2}}{\sum_{\lambda_1,\lambda_2=\pm} L^{\lambda_1\lambda_2}}$$

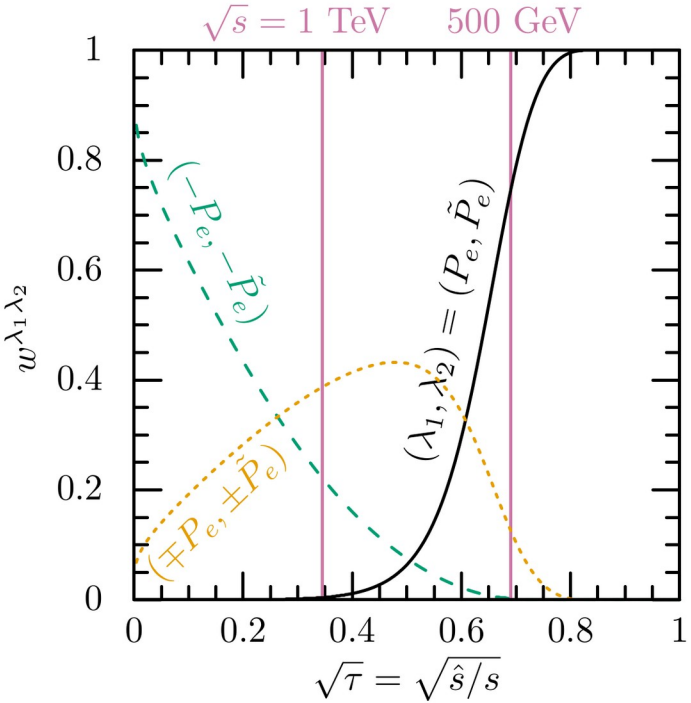

FIG. 2. *(Left) The helicity-dependent luminosities* $L^{\lambda_1\lambda_2} = \frac{1}{\mathcal{L}_{ee}} \frac{\mathrm{d}\mathcal{L}_{\gamma\gamma}^{\lambda_1\lambda_2}}{\mathrm{d}\sqrt{\tau}}$ *taking* $P_e P_c = \tilde{P}_e \tilde{P}_c = -1$ *and* $x = 4.8$. *From left to right,* $(\lambda_1, \lambda_2) = (+,+)$, $(-,-)$, $(-,+)$, *and* $(+,-)$ *while, from top to bottom,* $(P_e = -P_c, \tilde{P}_e = -\tilde{P}_c) = (+,+)$, $(-,-)$, $(-,+)$, *and* $(+,-)$. *In each frame, we also show the average luminosity* $\frac{1}{4}\sum_{\lambda_1,\lambda_2=\pm} L^{\lambda_1\lambda_2}$ *and the unpolarized one* $\frac{1}{\mathcal{L}_{ee}} \frac{\mathrm{d}\mathcal{L}_{\gamma\gamma}^{\mathrm{unp}}}{\mathrm{d}\sqrt{\tau}}$ *in dashed red and blue lines, respectively, for comparison. (Right) The weight functions* $w^{\lambda_1\lambda_2}$ *for* $(\lambda_1, \lambda_2) = (P_e, \tilde{P}_e)$ *(black solid),* $(\lambda_1, \lambda_2) = (-P_e, -\tilde{P}_e)$ *(green dashed), and* $(\lambda_1, \lambda_2) = (\mp P_e, \pm \tilde{P}_e)$ *(orange dotted). The vertical lines at* $\sqrt{\tau} = 0.345$ *and* 0.69 *mark the* $2M_t$ *threshold for* $\sqrt{s} = 1$ TeV *and* 500 GeV, *respectively.*

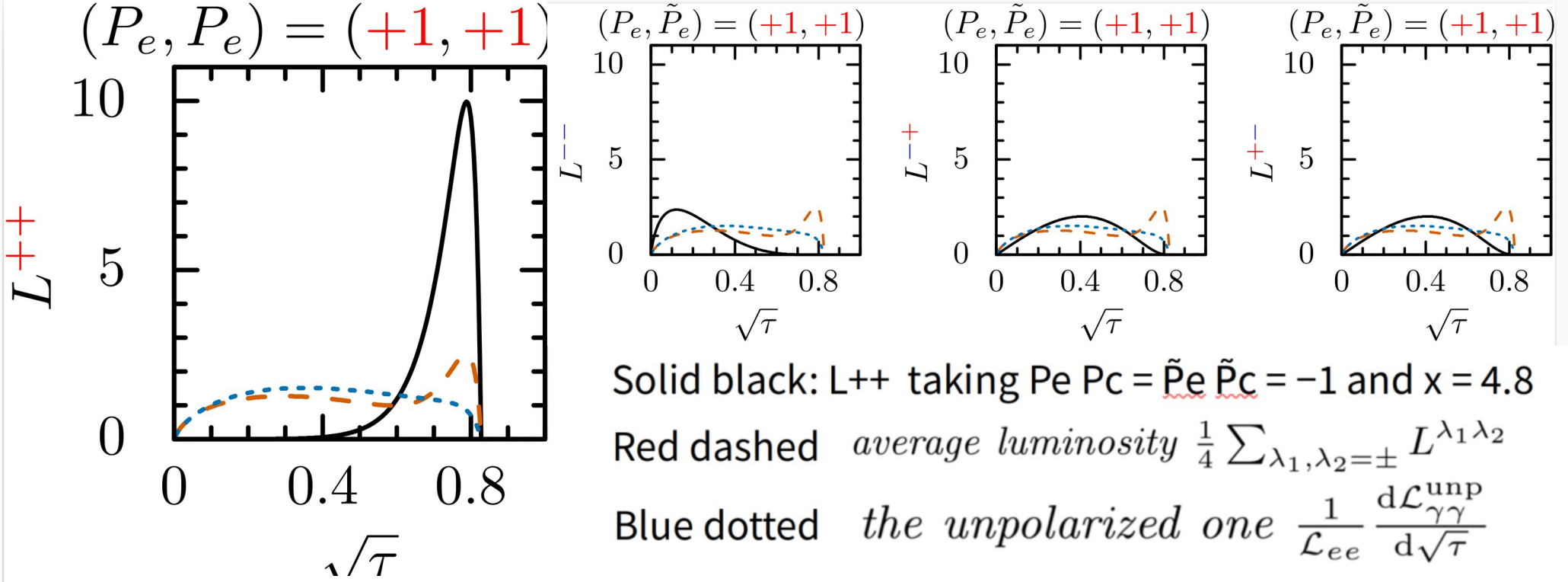

Solid black: L++ taking Pe Pc = P̃e P̃c = −1 and x = 4.8

Red dashed $\textit{average luminosity}\ \frac{1}{4}\sum_{\lambda_1,\lambda_2=\pm} L^{\lambda_1\lambda_2}$

Blue dotted $\textit{the unpolarized one}\ \frac{1}{\mathcal{L}_{ee}}\frac{\mathrm{d}\mathcal{L}_{\gamma\gamma}^{\mathrm{unp}}}{\mathrm{d}\sqrt{\tau}}$

$$\frac{1}{4}\sum_{\lambda_1,\lambda_2=\pm} L^{\lambda_1\lambda_2} = \frac{1}{4}\sum_{\lambda_1,\lambda_2=\pm}\frac{1}{\mathcal{L}_{ee}}\frac{\mathrm{d}\mathcal{L}_{\gamma\gamma}^{\lambda_1\lambda_2}}{\mathrm{d}\sqrt{\tau}} \xrightarrow{P_eP_c=\tilde{P}_e\tilde{P}_c=0} \frac{1}{\mathcal{L}_{ee}}\frac{\mathrm{d}\mathcal{L}_{\gamma\gamma}^{\mathrm{unp}}}{\mathrm{d}\tau} = \left.\frac{1}{\mathcal{L}_{ee}}\frac{\mathrm{d}\mathcal{L}_{\gamma\gamma}^{\lambda_1\lambda_2}}{\mathrm{d}\tau}\right|_{P_e=P_c=\tilde{P}_e=\tilde{P}_c=0}$$

average luminosity

unpolarized luminosity: independent of the colliding photon helicities

$$L^{\lambda_1\lambda_2} \equiv \frac{1}{\mathcal{L}_{ee}}\frac{\mathrm{d}\mathcal{L}_{\gamma\gamma}^{\lambda_1\lambda_2}}{\mathrm{d}\sqrt{\tau}}$$

weight functions

$$w^{\lambda_1\lambda_2} \equiv \frac{L^{\lambda_1\lambda_2}}{\sum_{\lambda_1,\lambda_2=\pm} L^{\lambda_1\lambda_2}}$$

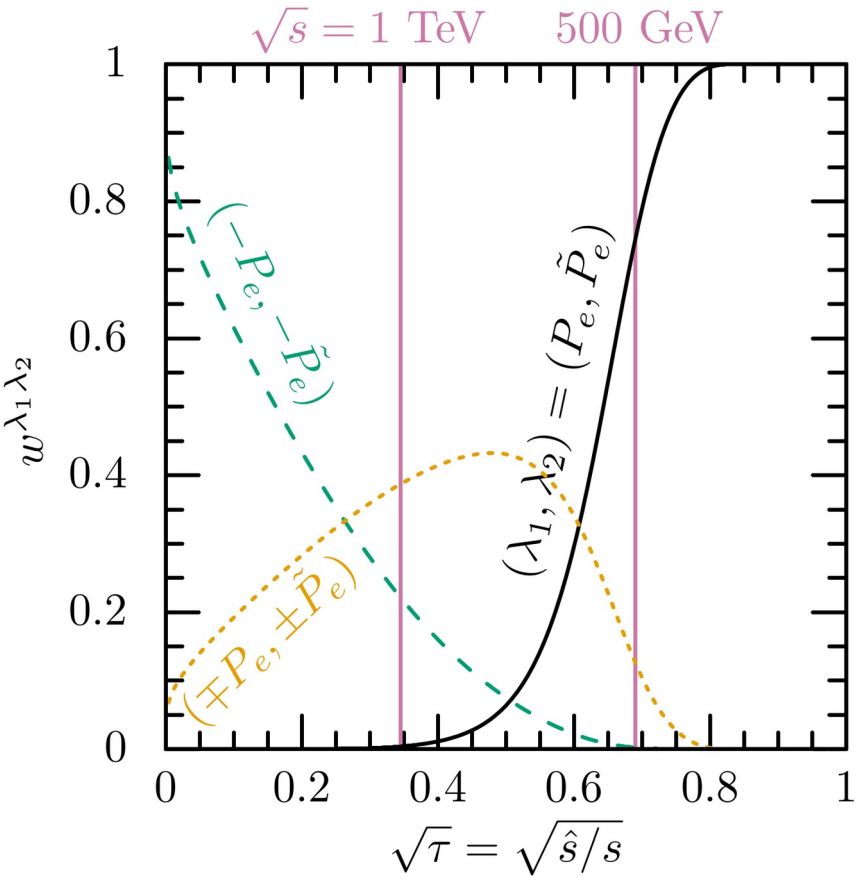

More than 70% of the colliding photons carry the helicities of the initial electron and positron beams within the kinematic region :

$$0.68 \lesssim \sqrt{\tau} \lesssim 0.82$$

This interval corresponds to

$$340\ (680) \lesssim \hat{s}/\text{GeV} \lesssim 410\ (820)$$

for sqrt(s) = 500 (1000) GeV, spanning energies near (well above) the $t\bar{t}$ threshold 2Mt .

Results

The spin density matrix is a function of cos Θ and $\hat{s}$ and, when they are given, one can calculate the entanglement quantifiers and identify the entangled/nonlocal regions once we know how to handle the spin density matrix with the colliding photons polarized

Spin density matrix with polarized colliding photons

The 16 polarization coefficients

$$\widehat{C}_i = \sum_{\lambda_1,\lambda_2=\pm} c_i^{\lambda_1\lambda_2}$$

$$\widehat{C}_1[+++] = \frac{1}{4}\sum_{\lambda_1,\lambda_2=\pm}\left[|\langle ++;\lambda_1\lambda_2\rangle|^2 + |\langle --;\lambda_1\lambda_2\rangle|^2\right]$$

The luminosity-weighted polarization coefficients

$$\widehat{C}_i^w \equiv \sum_{\lambda_1,\lambda_2=\pm} w^{\lambda_1\lambda_2}\, c_i^{\lambda_1\lambda_2}$$

$$w^{\lambda_1\lambda_2} \equiv \frac{L^{\lambda_1\lambda_2}}{\sum_{\lambda_1,\lambda_2=\pm} L^{\lambda_1\lambda_2}}$$

** unpolarized case: $w^{\lambda_1\lambda_2}$ = 1 / 4 all the same

** perfectly polarized case: $w^{\lambda_1\lambda_2}$ =1

only one is nonvanishing

The luminosity-weighted spin density matrix can be obtained by replacing each unweighted coefficient $\widehat{C}_i$ with its luminosity-weighted counterpart $\widehat{C}_i^w$

Unpolarized colliding photons: a reference

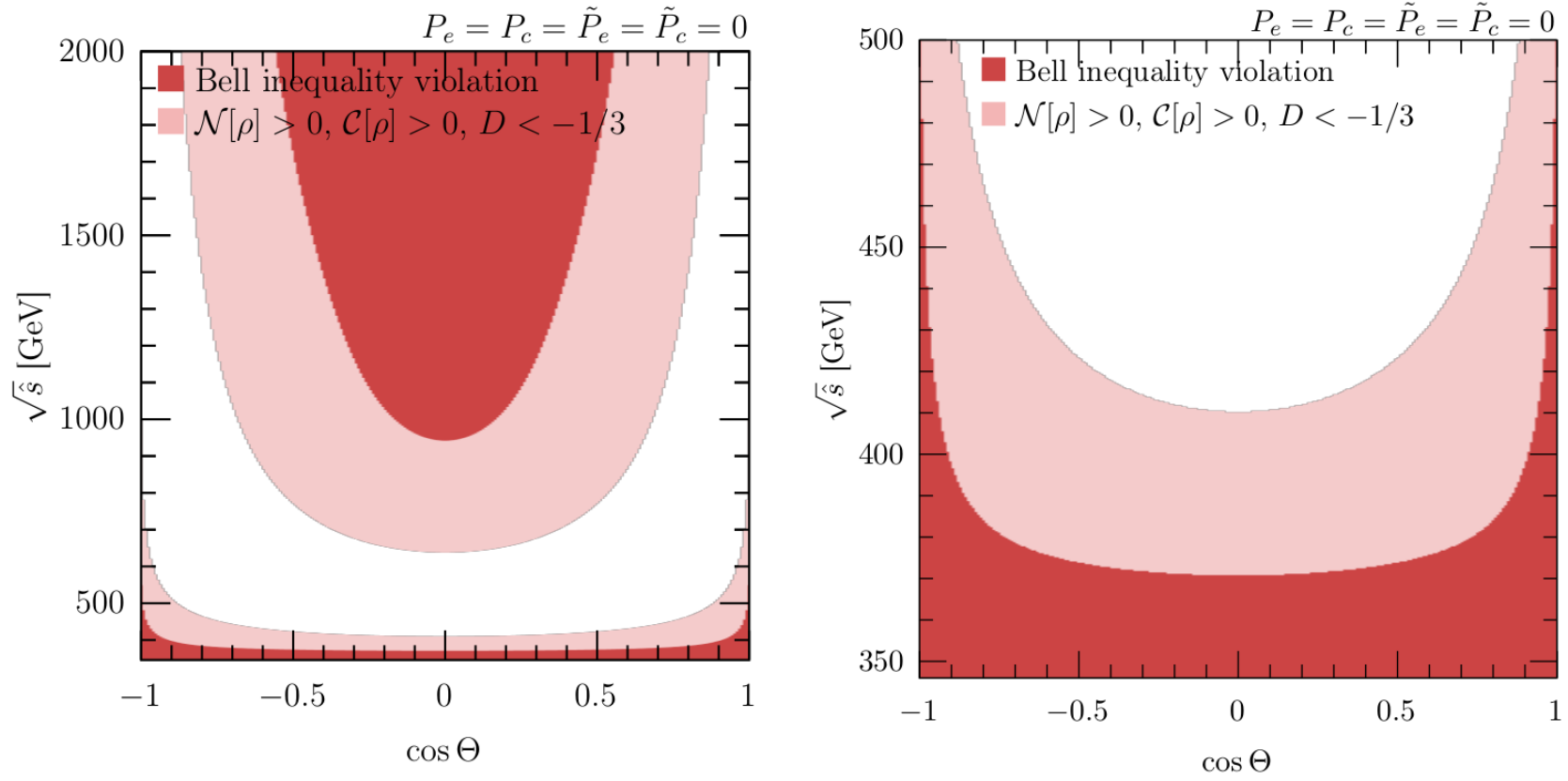

FIG. 3. **Quantum entanglement in the unpolarized case**: *(Left) Quantum entanglement for the unpolarized case* $P_e = P_c = \tilde{P}_e = \tilde{P}_c = 0$, *shown in the* $(\cos\Theta, \sqrt{\hat{s}})$ *plane. Shaded regions satisfy* $\mathcal{N}[\rho] > 0$, $\mathcal{C}[\rho] > 0$, *and* $D < -1/3$, *indicating entanglement of the* $t\bar{t}$ *spin state. The densely shaded red regions additionally satisfy* $m_{12} > 1$, *indicating violation of the Bell inequality. (Right) Magnified view of the region* $2M_t < \sqrt{\hat{s}} < 500$ *GeV.*

Polarized colliding photons with sqrt{s}= 500 GeV

$$\sqrt{s} = 500\ \text{GeV};\quad P_e = -P_c = \tilde{P}_e = -\tilde{P}_c = +1\,.$$

$$2M_t < \sqrt{\hat{s}} \lesssim 410\ \text{GeV},\qquad w^{++} \gtrsim 0.7,\ w^{+-} = w^{-+} \lesssim 0.15,\ \text{and}\ w^{--} \lesssim 3 \times 10^{-3}$$

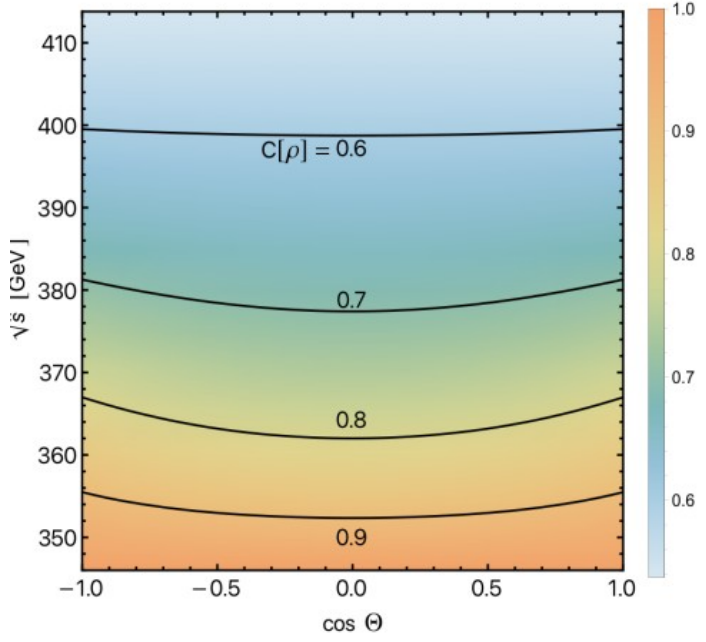

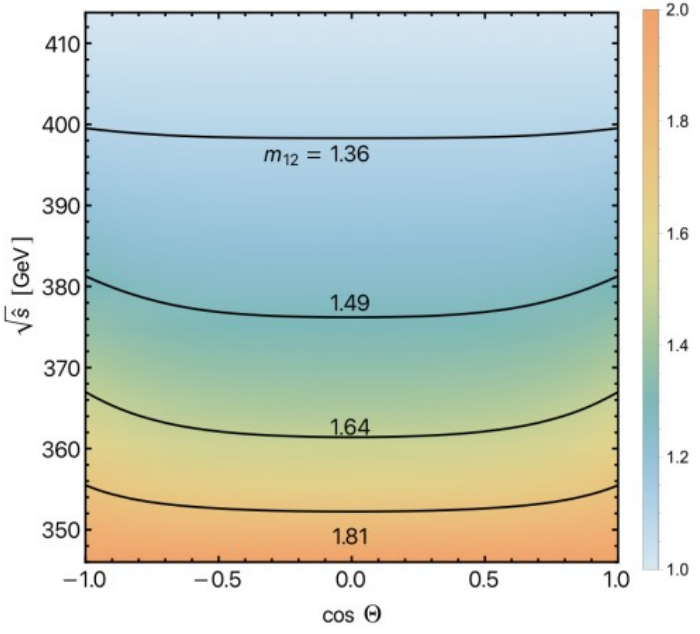

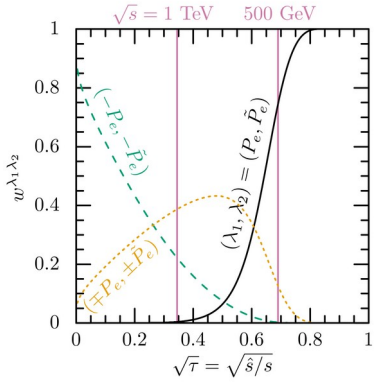

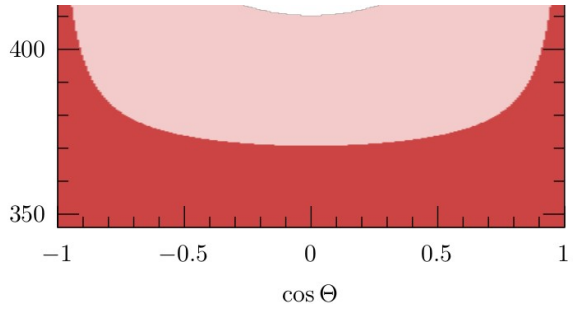

Quantum entanglement AND Bell nonlocality are observable throughout the entire (cos Θ, ŝ) plane!

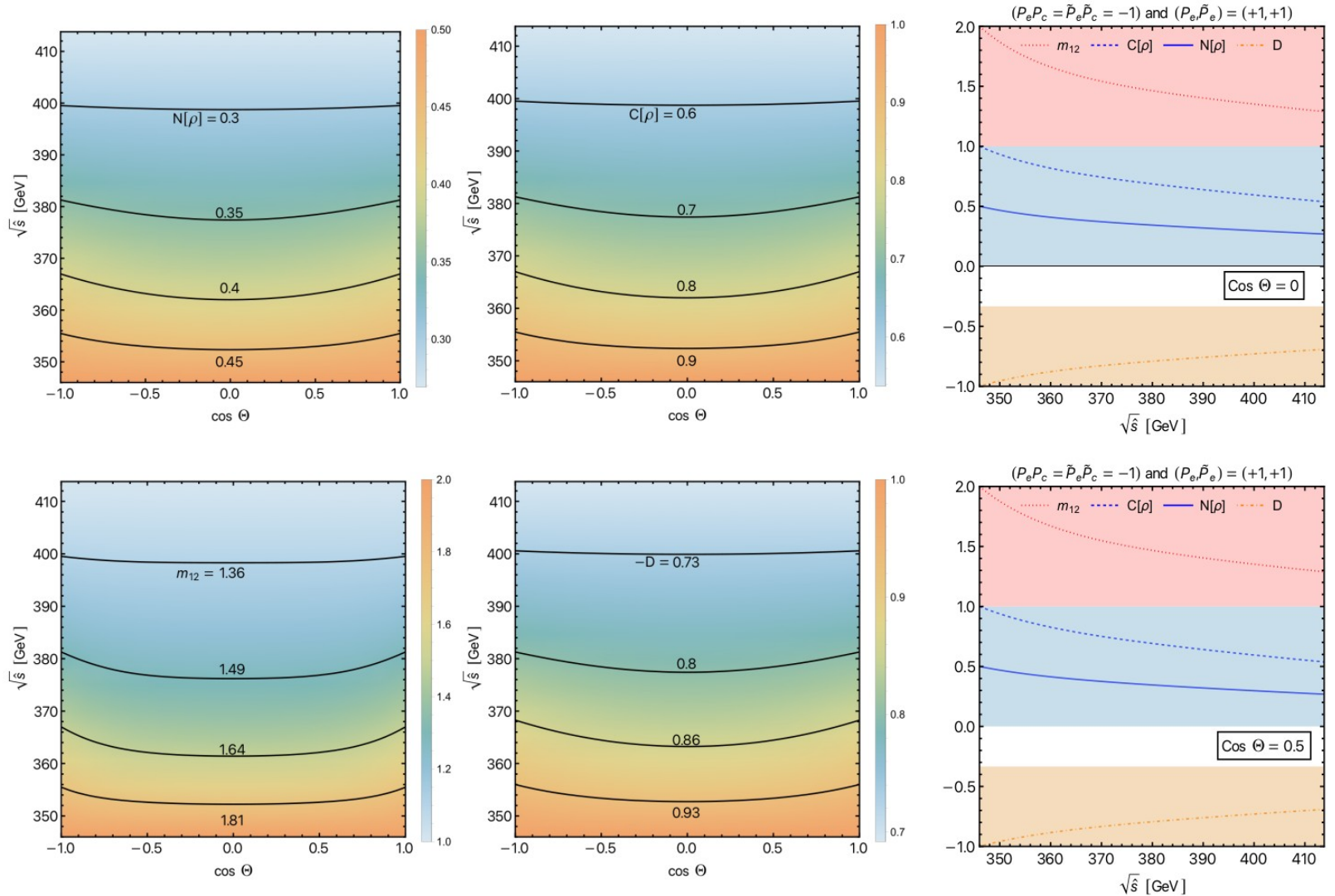

FIG. 6. **Quantum entanglement with $\sqrt{s} = 500$ GeV and $P_e = \tilde{P}_e = +1$**: *Same as in Fig. 5 but for* $\sqrt{s} = 500$ *GeV and* $P_e = -P_c = \tilde{P}_e = -\tilde{P}_c = +1$.

Polarized colliding photons with sqrt{s}= 1 TeV

$$\sqrt{s} = 1\ \text{TeV}; \quad P_e = -P_c = -\tilde{P}_e = +\tilde{P}_c = +1\,.$$

$$2M_t < \sqrt{\hat{s}} \lesssim 820\ \text{GeV} \qquad w^{+-} \lesssim 0.01,\ w^{++} = w^{--} \sim 0.4,\ \text{and}\ w^{-+} \sim 0.2$$

$$w^{+-} \gtrsim 0.7,\ w^{++} = w^{--} \lesssim 0.15,\ \text{and}\ w^{-+} \lesssim 3 \times 10^{-3}$$

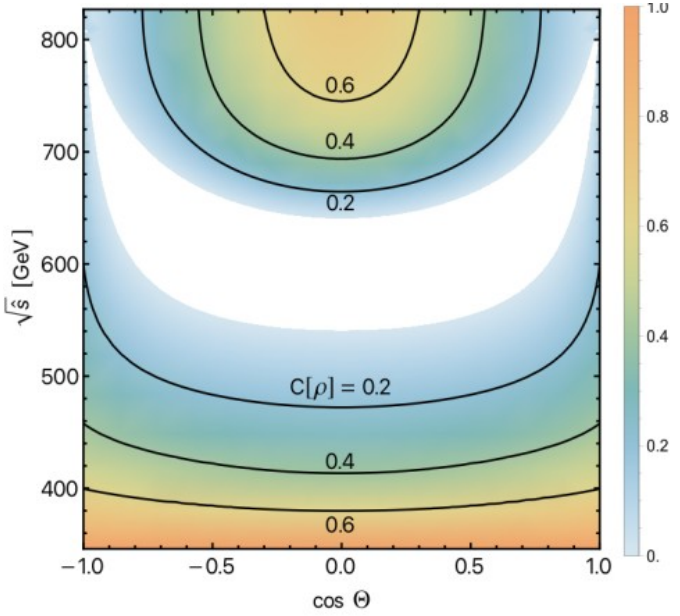

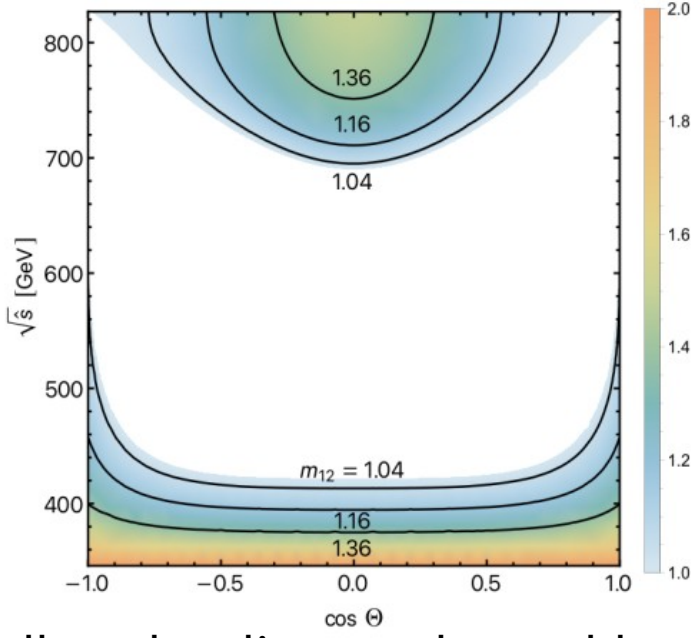

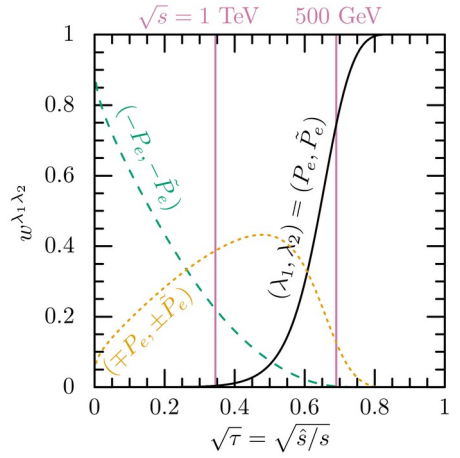

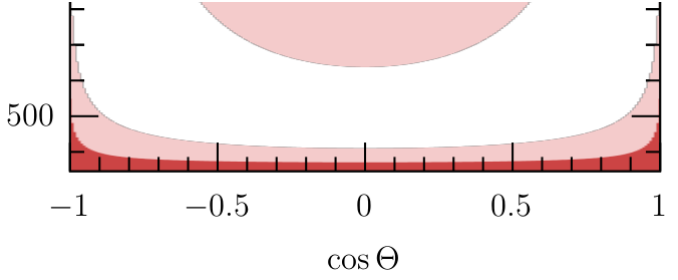

Quantum entanglement and Bell nonlocality are observable throughout the broader (cos Θ, ŝ) region !

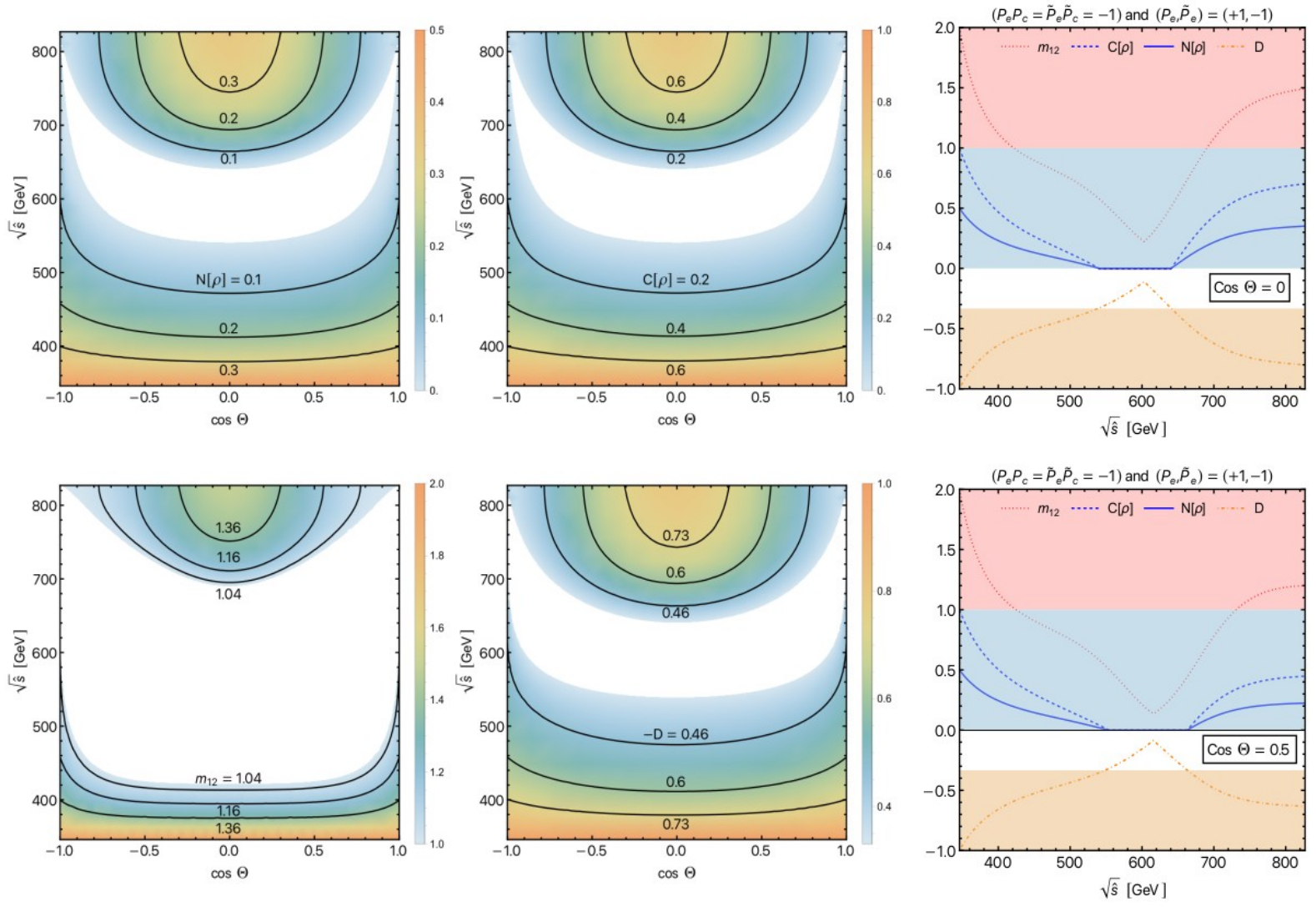

FIG. 7. **Quantum entanglement with $\sqrt{s} = 1$ TeV and $P_e = -\tilde{P}_e = +1$**: *Same as in Fig. 6 but for* $\sqrt{s} = 1$ *TeV and* $P_e = -P_c = -\tilde{P}_e = \tilde{P}_c = +1$.

Comparisons:

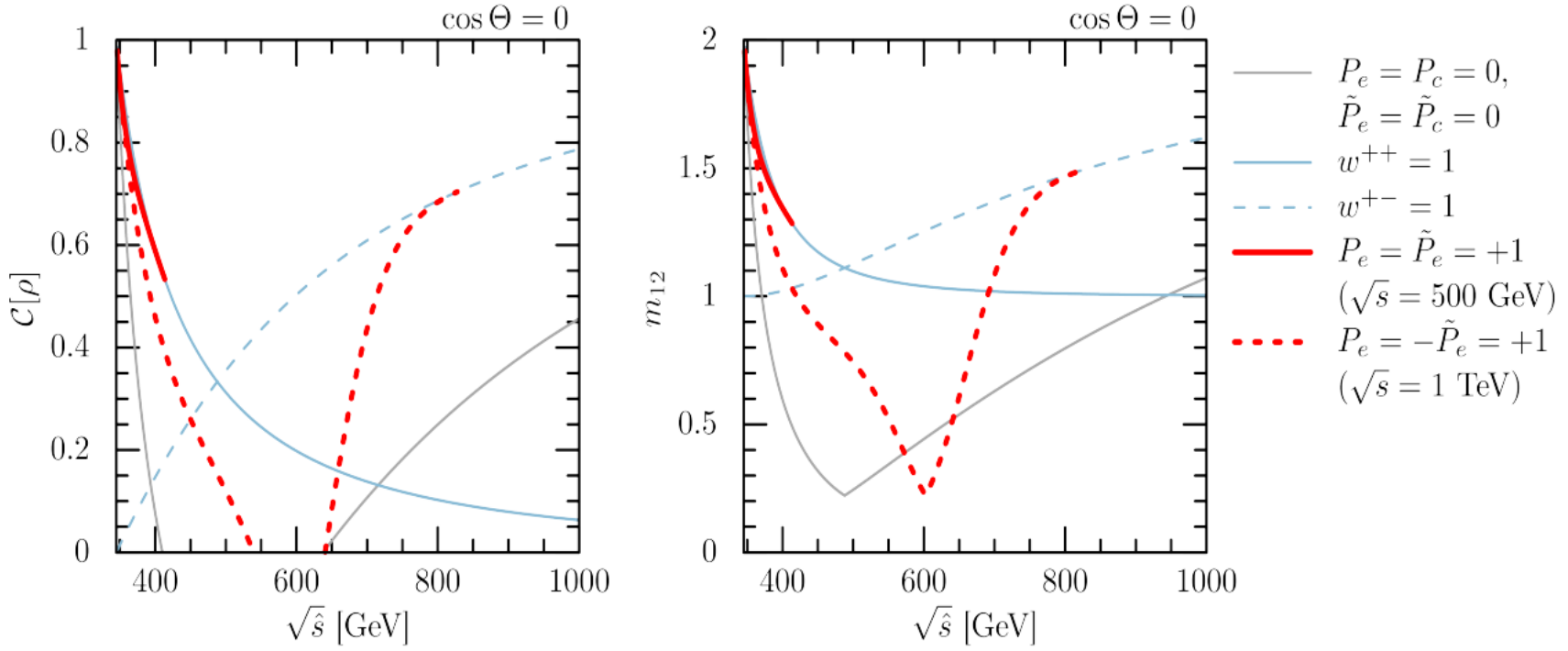

FIG. 8. **Comparisons of quantum entanglement and Bell inequality violation**: *Concurrence $\mathcal{C}[\rho]$ (left) and Bell nonlocality parameter m_{12} (right) as functions of $\sqrt{\hat{s}}$ at $\cos\Theta = 0$ for unpolarized photons with $P_e = P_c = \tilde{P}_e = \tilde{P}_c = 0$ (black solid), perfectly polarized same-helicity photons (blue solid), and perfectly polarized opposite-helicity photons (blue dashed). Thick solid and dashed red curves correspond to $P_e = -P_c = \tilde{P}_e = -\tilde{P}_c = +1$ ($\sqrt{s} = 500$ GeV) and $P_e = -P_c = -\tilde{P}_e = +\tilde{P}_c = +1$ ($\sqrt{s} = 1$ TeV), respectively.*

Conclusions

A photon linear collider is an ideal machine to probe quantum entanglement and Bell nonlocality thanks to its capability to control the polarizations of the colliding photons which can significantly enhance the magnitudes of the quantum entanglement quantifiers.